JREE: Vol. 2, No.2, (Spring 2015) 29-35

Journal of Renewable Energy and Environment

Research Article

Journal Homepage: www.jree.ir

Further Improvement in Efficiency of ZnO Nanorod Based Solar Cells Using ZnS Quantum Dots as Light Harvester and Blocking Layer Material

M. Mehrabian*, S. Aslyousefzadeh

Department of Basic Science, University of Maragheh, Maragheh, Iran

PAPER INFO

Paper history:
Received 22 November 2014
Accepted in revised form 02 June 2015

Keywords:
ZnO nanorods
ZnS quantum dots
hydrothermal method
growth period
Spin-assisted SILAR technique
Solar cell

ABSTRACT

Zinc oxide nanorod arrays (ZnO NRs) were grown on the ZnO seed layers via an aqueous solution using hydrothermal method and their photovoltaic properties were investigated. It was found that the growth period of 20 minutes is the optimum condition for ZnO nanorods growth, the cell containing these nanorods was considered as a reference cell. In order to further increase the cell performance, ZnS quantum dots (QDs) were fabricated on the ZnO NRs (reference cell) by SILAR technique with different number of cycles. The effect of the number of SILAR cycle (n) on structural and photovoltaic properties was studied. The optimum number of SILAR cycles for ZnS QDs was obtained (n=4). Experimental results showed that using ZnS QDs as light absorber material is an effective way to improve device performance. Morphology, crystalline structure and optical absorption of layers were analyzed by a scanning electron microscope (SEM), X-ray diffraction (XRD) and UV-Visible absorption spectra, respectively. The maximum power conversion efficiency of 3.59% in the inverted configuration of ITO/ZnO film/ZnO NR(20)/ZnS(n) QDs/P3HT/PCBM/Ag hybrid solar cell was achieved for a device based on ZnS(4) under an illumination of one Sun (AM 1.5G, 100 mW/cm2).

1. INTRODUCTION

Photovoltaic (PV) devices attract great attention owing to the growing demands for clean and renewable energy. Low-cost fabrication methods are of the major interest to reduce production costs of PV devices. Recently, using nanostructures (such as nanowires and nanorods) has extensively been studied for solar cells applications [1-7].

Different wide band gap metal oxides, such asTiO_2, ZnO, SnO_2, and Nb_2O_5 have been frequently tested for photovoltaic properties [8-10]. Among these materials, ZnO has attracted much attention in fabrication of solar cells due to its excellent properties such as low cost, direct band gap (3.37 eV), high exciton energy (60 m eV), high electron mobility (200 $cm^2\ V^{-1}\ s^{-1}$), non toxicity abd good air stability [11-13].

Environmentally friendly and low-cost ZnO nanorod array is particularly well suited for solar cell application as they can be easily grown on different substrates by different physical and chemical techniques, such as metal–organic, chemical vapor deposition, magnetron sputtering, vapor liquid solid, chemical vapor deposition, and hydrothermal method [14-19].

Among these methods, the hydrothermal technique is the best one due to its simplicity, low temperature, low cost, reproducible and able to control the length and diameter of nanorods by varying experiment conditions such as time and concentration of precursors. In addition to an increased charge carrier collection in 1-dimensional structures of ZnO (e.g. nanorods), they possess the potential of enhanced light absorption [20, 21].

It has been reported that ZnO nanorods in solar cells improve light absorption and charge carrier collection [22-26]. Employing semiconductor nanoparticles (or quantum dots) as sensitizers in solar cells has two special advantages. First and foremost, the size quantization effect allows one to tune the band energy and visible response by simply varying the QD size [27, 28]. Another advantage is that QDs open new ways to utilize hot electrons or generate multiple electron–hole pairs with one single proton through the impact ionization effect [29].

Zinc sulfide (ZnS) is an important II-VI semiconductor inorganic compound which exists in two main crystalline forms (cubic and hexagonal). It has a direct band gap of 3.6 eV (bulk) at 300 K [30, 31]. ZnS is a

*Corresponding Author's Email: masood.mehrabian@yahoo.com (M. Mehrabian)

promising material for optoelectronic device applications such as blue light emitting diodes, modulators, electroluminescent devices and photovoltaic cells. It has been extensively studied and most importantly, it is a nontoxic and is more environmentally friendly material [32-34]. ZnS QDs can be fabricated by using various techniques such as spray pyrolysis, chemical bath deposition (CBD), successive ionic layer adsorption and reaction (SILAR) and so on.

SILAR method which is known as modified version of chemical bath deposition (CBD) is a simple, low cost, versatile, less time-consuming and large-scale production technique for the deposition of quantum dots. A variety of substrates such as insulators, semiconductors, metals and temperature sensitive substrates (like polyester) can be used since the deposition is carried out at or near to room temperature [35].

SILAR method can be done during either spin-coating or dip-coating processes. The process based on spin-coating is denoted spin-SILAR to distinguish it from the conventional SILAR method based on dip-coating (dip-SILAR). The spin- SILAR or spin- assisted SILAR method involves the layer-by-layer build up of a quantum dot film via the successive adsorption and reaction of anions and cations by spin-coating. Because the adsorption, reaction, and rinsing steps occur simultaneously during spin coating, spin-SILAR does not require rinsing steps, making the growth process simpler and faster than in the dip-SILAR technique [36].

In present work, ZnO nanorod arrays (ZnO NRs) were synthesized using a hydrothermal method and in order to further increase the cell performance, ZnS QDs as light absorber material were synthesized on these nanorods via spin assisted SILAR technique. The spin assisted SILAR process eliminates the rinsing of excessive precursors and the additional drying process in conventional SILAR methods. The influence of number of SILAR cycles on the photovoltaic properties of fabricated solar cells with structure of ITO/ZnO film/ZnO nanorods/ZnS QDs/P3HT/PCBM/Ag was investigated.

2. EXPERIMENTAL DETAILS

2. 1. Deposition of ZnO seed layer All devices were prepared on ITO-patterned glass substrates. Prior to depositing ZnO seed layer, these substrates were ZnS QDs) and fabricated photovoltaic devices containing ZnO NRs covered by ZnS QDs.

3. RESULTS AND DISCUSSION

3. 1. Optimizing the growth period of ZnO NRs without ZnS QDs (the reference cell) To optimize the growth period of ZnO nanorods, first of all and in the absence of ZnS QDs, the growth period of NRs were varied, and the photovoltaic properties of devices with structure of ITO/ZnO film/ZnO NRs/P3HT/PCBM/Ag were recorded. The relationship between growth period of ZnO NRs and cell efficiency is shown if Figure 2(a).

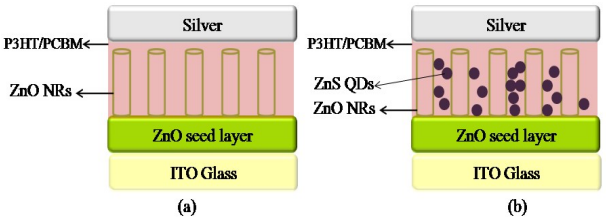

Figure 1. Schematic view of a (a) reference cell and (b) solar cells containing ZnS QDs.

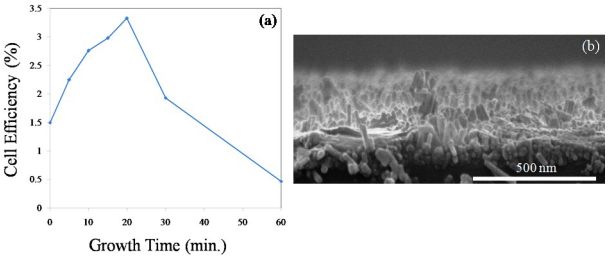

Figure 2. (a) The variation of cell efficiency with growth time, (b) SEM image of ZnO nanorods grown for 20 min (NR20).

As it can be seen from Figure 2(a). the maximum power conversion efficiency of 3.33% was obtained for a cell containing ZnO nanorods grown for 20 min which will be considered as the reference cell. The cross sectional image of these nanorods with an average length of 120 nm is shown in Figure 2(b).

3.1.1. Characterization of ZnO seed layer and nanorod arrays The photovoltaic (PV) properties of reference cell with structure of ITO/ZnO film/ZnO NR20/P3HT/PCBM/Ag were investigated. In Figure 3(a). the J–V characteristic of this solar cell is shown. The active area of device was 6 mm^2. The XRD spectra of the ZnO seed layer and ZnO nanorod arrays are shown in Figure 3(b).

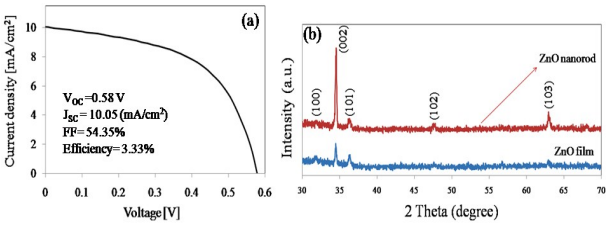

Figure 3. (a) J–V characteristics of reference solar cell based on ZnO NR(20), (b) XRD patterns of ZnO seed layer and ZnO nanorod arrays.

The crystalline nature of ZnO nanorods can be well indexed to known structures of hexagonal (wurtzite)

ZnO, with lattice constants a=0.32498 nm, b=0.32498 nm and c=5.2066 nm [JCPS cardno.36-1451]. Five significant wurtzite ZnO diffraction peaks, (100), (002), (101), (102) and (103) appear at 2θ= 31.8°, 34.4°, 36.2°, 47.6° and 62.7°, respectively. These results are in agreement with those of other authors [38].

It is evident that the (002) peak intensity of ZnO seed layer is lower than that of NRs. This strongly enhanced (002) diffraction peak in Figure 3(b). at about 34.4° indicates preferential growth of ZnO NRs along the c-axis [18, 39]. Moreover, the growth rate of ZnO along c-axis is faster than those of other orientations because the basal plane (001) has the highest surface energy [40, 41].

3. 2. Further increasing the cell performance

To promote the cell performance, ZnS quantum dots (QDs) were used as light harvester and blocking layer material in device. Such structure can be called a quantum dot sensitized solar cell (QDSSC).

The application of QDs in solar cells may help to develop solar cells with energy conversion efficiencies above the Shockley–Queisser [42] limit (for solar cells with a single band gap). The high potential of QDs for large solar energy conversion efficiency as well as possible configurations of QD solar cells were discussed by Nozik [43].

The function of a QDSSC is based on the formation of electron-hole pair (exciton) in nanoparticle semiconductor by absorbing the incident light. Figure 4. shows the schematic diagram of exciton generation and charge transfers to different layers and corresponding energy level diagram for (a) reference cell and (b) other cells in our experiment. The situation of electronic energy levels is the most important factor governing efficient electron transfer between two semiconductors (and, consequently, photocurrent generation) [44].

Devices are irradiated from ITO side. In the reference cell, the P3HT absorbs light and electron-hole pairs are generated over this layer (Figure 4(a)). To extract the electric energy, these excitons must be dissociated at interfaces and generated electrons have to be transferred to (ZnO layer) an electron conducting layer in a properly way before they recombine with holes (the arrow shown in Figure 4). While the photo-generated holes must be extracted by (P3HT/PCBM), a hole conducting layer, toward silver contact. The strategy to separate electron and hole pairs into the neighboring layers can be achieved by choosing materials with appropriate energy levels [45].

To prevent the recombination (electrons in ZnO with holes in P3HT/PCBM), a blocking layer of ZnS QD was deposited between ZnO and P3HT/PCBM (Figure 4(b)). As it can be seen from Figure 4(b), in this situation, the energy levels of components [46, 47] create a cascade structure between ITO/ZnO/ZnS/P3HT/PCBM which facilitates charge transfer from ZnS QDs to ITO contact. In this structure, ZnS QD layer absorbs the light and blocks the recombination in the ZnO & P3HT/PCBM interface.

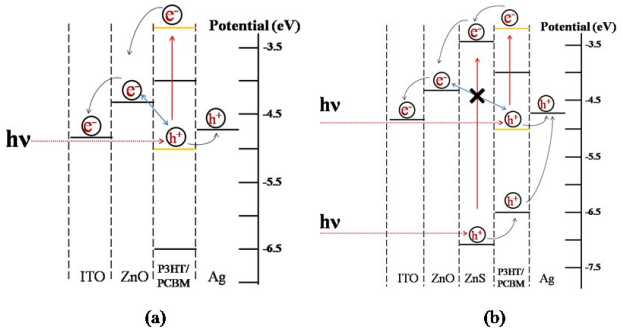

Figure 4. Energy levels and charge transport mechanism in (a) reference cell and (b) other cells containing ZnS QDs.

3. 3. Absorption spectra

To investigate the quantum confinement effect of ZnS QDs, the optical absorption spectra of ZnS QD with various SILAR cycles (n) over the range of 0.32–0.40 μm are shown in Figure 5. The spectra exhibit a peak in the short-wavelength region (350-370 nm) for each sample. The intensities of the absorption peak increases with the SILAR cycle (n). These absorption peaks can be attributed to the excitonic excitations associated with the band structure of ZnS. The increasing absorption suggests the increased number of QDs deposited on the substrate.

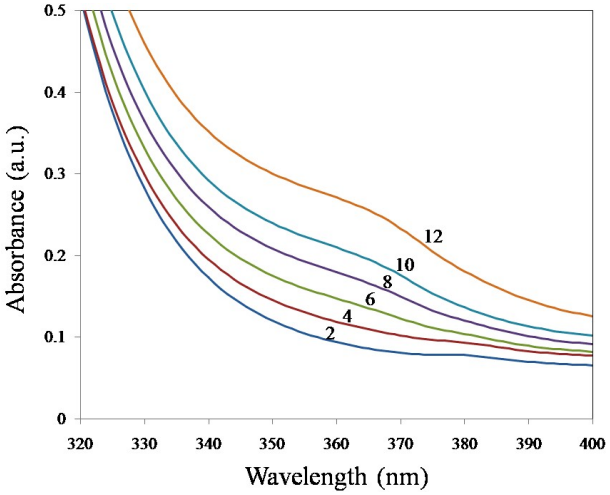

Figure 5. Absorption spectra of ZnS QDs on glass substrates. The labels beside the curves indicate the number SILAR cycles (n).

Band gap energy of the ZnS(n) can be calculated by plotting $(\alpha h\nu)^2$ versus hν, as shown in Figure 6. It is clear that by increasing (n), the band-gap energy of the ZnS quantum dots slightly decreases from 3.70 eV (for n=2) to 3.38 eV (for n=12).

Extrapolations in Figure 6. show a reduction in the band-gap energy (red- shift), which suggest that more number of ZnS nanoparticles are gathered on substrate,

their aspect ratio increases, and this leads to a red shift of the absorption peak [48].

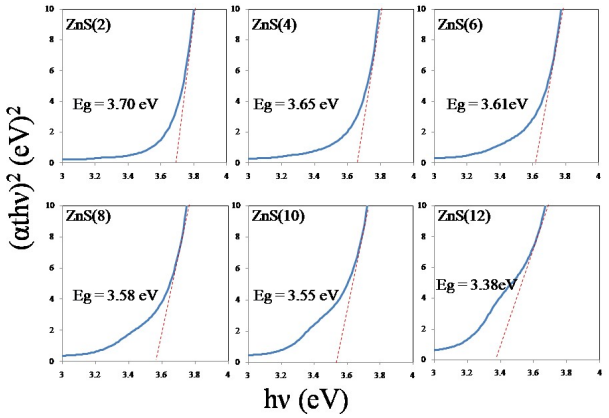

Figure 6. Optical band-gap energy (*E*g) of the ZnS QDs with various SILAR cycles (n).

3. 4. Characterization of ZnS QDs Diffraction patterns of ZnS QDs are shown in Figure 7. All the diffraction peaks from (111), (200), (220) and (311) respectively at 2θ= 28.9°, 33.5°, 48.1° and 57.1° are associated with reflections of the cubic zinc blende phase (sphalerite) of ZnS and are in agreement with other reports [49, 50].

These peaks were identified by using JCPDS (reference code: 01-080-0020) data for ZnS. The central broad hump is due to the amorphous glass substrate. The lattice parameters of the cubic structure are equal to a= b=c=5.345 A˚. The presence of broad peaks in XRD implies presence of smaller particles [52].

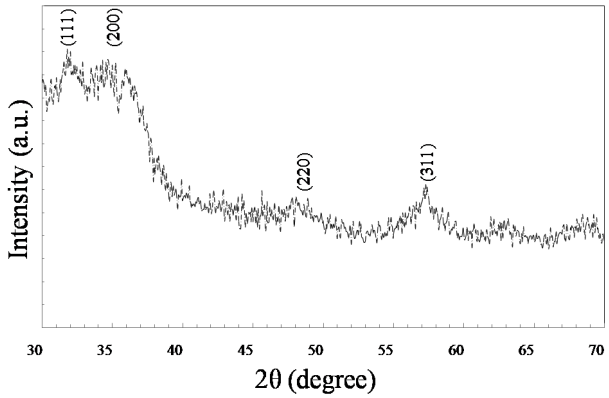

Figure 7. XRD patterns of ZnS quantum dots deposited on bare glass substrate.

3. 5. Surface morphology The surface morphology of ZnO NRs grown for 20 min (NR20) on the ZnO layer without ZnS QDs (reference cell) and ZnO NR20 covered with ZnS QDs with different cycles (n) are shown in Figure 8.

It is clear from Figure 8. that in reference cell (Figure 8. (a)), there are void spaces between ZnO nanorods and the tip of nanorods are separated. But deposition of ZnS QD layer on top of nanorods gradually fills these void spaces. On the other hand, repeating the number of cycles in spin assisted SILAR technique leads to change in size, density and morphology of deposited ZnS QDs. So that for n=2 (Figure 8(b), thickness ~ 16 nm), ZnS particles are deposited separately in the space of between nanorods, and no aggregation is observed. For n=4 (Figure 8(c)), the average thickness of ZnS QDs is 24 nm and ZnS QDs can still penetrate in the space between NRs. But for n>4, the whole area of nanorods are covered by ZnS QDs (Figure 8(e, f)), QDs are stacked on each other and make a nearly smooth and compact layer. These images suggest that ZnS QD (n=4) provides optimal surface morphology and device performance.

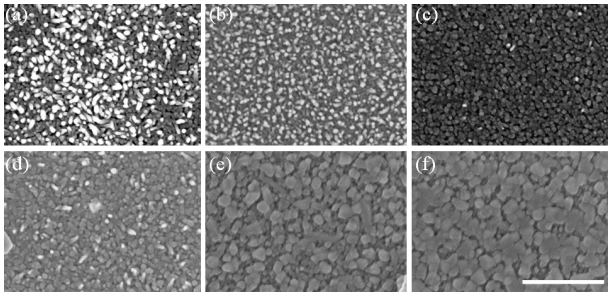

Figure 8. Plan-view FE-SEM images of ZnO NRs grown for 20 min (a) without ZnS QD (reference cell), covered by ZnS QDs with (b) 2, (c) 4, (d) 6, (e) 8 and (f) 10 SILAR cycles. Scale bar: 500 nm.

3. 6. Photovoltaic properties of samples The photovoltaic (PV) properties of samples were investigated. In Figure 9. the J–V characteristics of solar cells based on ZnO nanorods grown for 20 min and cover by ZnS QDs for different number of SILAR cycles are compared. All the devices are fabricated with the same active area of 6 mm^2.

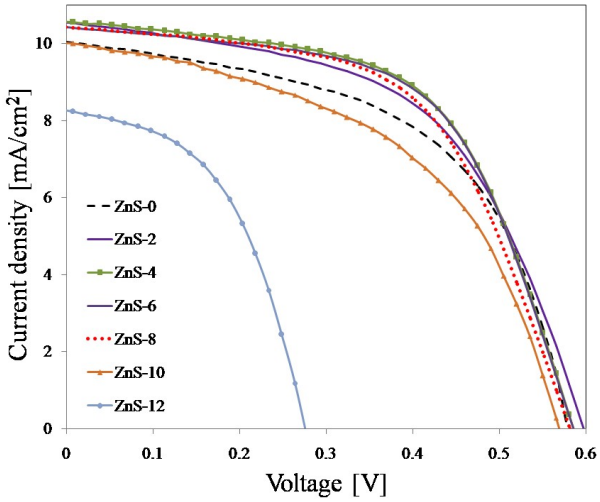

Figure 9. J–V characteristics of solar cells based on ZnO nanorods grown for 20 min and covered with ZnS QDs. Solar cells illuminated at 100 mW/cm^2; the active area is 6 mm^2.

From the J–V characteristics, a clear performance enhancement was observed in the device based on ZnO

NR20 covered with ZnS(4). For this device, the short circuit current (Jsc), open circuit voltage (Voc), fill factor (FF) and efficiency were all improved. The detailed values of these parameters are given in Table 1.

TABLE 1. Photovoltaic performance of solar cells based on ZnO nanorods grown for 20 min and covered with ZnS QDs (100 mW/cm^2 and AM 1.5 simulated solar light).

Electrode	V_{OC} (V)	J_{SC} (mA/cm^2)	FF (%)	Efficiency (%)
Reference cell	0.58	10.05	54.35	3.33
ZnS(2)	0.60	10.62	53.60	3.40
ZnS(4)	0.59	10.64	57.57	3.59
ZnS(6)	0.59	10.43	58.33	3.56
ZnS(8)	0.58	10.42	56.70	3.44
ZnS(10)	0.57	10.01	49.80	2.91
ZnS(12)	0.27	8.26	49.54	1.12

In this study, the reference cell with ITO/ZnO film/ZnO NR20/P3HT/PCBM/Ag structure as shown in Figure 1(a). has an open-circuit voltage, a short-circuit current density and power conversion efficiency of 0.58 V, 10.05 mA/cm^2 and 3.33%, respectively. To improve the cell performance, ZnS QDs with different number of SILAR cycles (n) were deposited on the nanorod arrays. At the beginning of the deposition of ZnS QDs, SILAR process is supposed to increase the coverage ratio of ZnS on the surface of ZnO nanorods by replenishing the uncovered area and the thickness of ZnS QD layer increases with the increase the number of SILAR cycles (ZnS(n)). Such increment of ZnS loading leads to more excited electrons under the illumination of light, which is advantageous to the photocurrent. Compared to the reference cell, photovoltaic parameters increase when nanorods are covered by ZnS (2). This improvement can be described as below. The light absorption is enhanced by using ZnS QD layer. In such device, both P3HT and ZnS layers absorb the incident light. As a result, J_{SC}, V_{OC} and efficiency are improved. On the other hand, ZnS QDs act as a blocking layer which decreases electron-hole recombination in the ZnO & P3HT/PCBM interface, as shown in Figure 4(b).

As it was mentioned, an optimized thickness of ZnS QD layer was obtained for n=4, which results in a highest Jsc, FF and efficiency by providing a good interfacial structure between ZnO and P3HT/PCBM layers and reducing the recombination of the injected electrons from ZnO to P3HT/PCBM due to a well-covered ZnS on the ZnO nanorods.

Maximum efficiency (3.59%) was obtained for 4 SILAR cycles (ZnS (4)). The higher efficiency of this device is attributed to its broader light absorption range which leads to a higher Jsc (10.64 mA/cm^2) compared with that of other ones.

However, as the thickness of ZnS QD layer further increases, it becomes darker, so the incident light cannot reach to P3HT layer, meanwhile, it will be more difficult to transport an electron from the ZnS QD layer into the ZnO film, leading to unfavorable electron transportation at ZnO/ZnS/P3HT/PCBM interface.

A slight reduction in Jsc was observed in solar cells with further increasing number of SILAR cycles (n>4) due to the aggregation of the quantum dots on top of nanorods as explained earlier. Meanwhile, the FF of device containing ZnS (4) is smaller than that of ZnS (6), probably due to the low driving force for the electron injection.

4. CONCLUDING REMARKS

In present study, ZnS QDs were prepared using SILAR technique with different SILAR cycles (n) on ZnO nanorod arrays. The photovoltaic properties of these cells with ITO/ZnO film/ZnO NR/ZnS(n)/P3HT/PCBM/Ag structure were compared to that of the reference cell with ITO/ZnO film/ZnO NR/P3HT/PCBM/Ag structure. Without using ZnS QDs, the maximum efficiency of 3.33% was obtained for the reference cell. While for devices containing ZnS QDs, the highest power conversion efficiency of 3.59% was achieved for ZnS (4). This improvement of photovoltaic properties has 2 main reasons. First, the light absorption is enhanced by using ZnS QD layer, and second, superior ability of ZnS QD layer in inhibiting the charge recombination at the ZnO and P3HT/PCBM interface. The results further indicated that using ZnS QD layer beside ZnO nanorod arrays has a significant effect on solar efficiency.

REFERENCES

1. Yuan, Z.L., Tao, S.L., Yu, J.S. and Jiang, Y.D., "Optical properties of 4 (Dicyanomethylidene)-6-(4-dimethylaminostyryl)-2-methyl-4H-pyran nanoparticles prepared by reprecipitation", ***Chemistry Letters,*** Vol. 39, No. 3, (2010), 302-303.
2. Yu, J.S., Yuan, Z.L. Xie, G.Z. and Jiang, Y.D., "Preparation, properties, and applications of low-dimensional molecular organic nanomaterials", ***Journal of Electronic Science and Technology,*** Vol. 8, No. 1, (2010), 3-9.
3. Huang, Q., Fang, L., Chen, X. and Saleem, M., "Effect of polyethyleneimine on the growth of ZnO nanorod arrays and their application in dye-sensitized solar cells", ***Journal of Alloys and Compounds,*** Vol. 509, No. 39, (2011), 9456– 9459.
4. Garnett, E.C. and Yang, P., "Silicon nanowire radial p-n junction solar cells", ***Journal of the American Chemical Society,*** Vol. 130, No. 29, (2008), 9224–9225.
5. Law, M., Greene, L.E., Johnson, J.C., Saykally, R. and Yang, P., "Nanowire dye-sensitized solar cells", ***Nature Materials,*** Vol. 4, (2005), 455–459.
6. Zhong, M., Yang, D., Zhang, J., Shi, J.Y., Wang, X.L. and Li, C., "Improving the performance of CdS/P3HT hybrid inverted solar cells by interfacial modification", ***Solar Energy Materials and Solar Cells,*** Vol. 96, (2012), 160–165.

7. Myung, Y., Kang, J.H., Choi, J.W., Jang, D.M. and Park, J., "Polytypic ZnCdSe shell layer on a ZnO nanowire array for enhanced solar cell efficiency", ***Journal of Materials Chemistry,*** Vol. 22, (2012), 2157–2165.
8. Sayama, K., Sugihara, H. and Arakawa, H., "Photo-electrochemical properties of aporous Nb2O5 electrode sensitized by a ruthenium dye", ***Chemistry of Materials,*** Vol. 10, (1998), 3825–3832.
9. Ferrere, S., Zaban, A. and Gregg, B.A., "Dye sensitization of nano-crystalline tin oxide by perylene derivatives", ***Journal of physical Chemistry B,*** Vol. 101, (1997), 4490–4493.
10. Keis, K., Lindgren, J., Lindquist, S.E. and Hagfeldt, A., "Studies of the adsorption process of Ru complexes in nanoporous ZnO electrodes", ***Langmuir,*** Vol. 16, (2000), 4688–4694.
11. Yang, P., Yan, H., Mao, S., Russo, R. J. Johnson, Saykally, R., Morris, N., Pham, J., He, R. and Choi, H.J., "Controlled Growth of ZnO Nanowires and Their Optical Properties", ***Advanced Functinal Materials,*** Vol. 12, No. 5, (2002), 323-331.
12. Xia, J.B. and Zhang, X.W., "Electronic structure of ZnO wurtzite quantum wires", ***The Europen Physical Journal B,*** Vol. 49, (2006), 415-420.
13. Baruah, S. and Dutta, J., "Hydrothermal growth of ZnO nanostructures", ***Science and Technology of Advanced Materials,*** Vol. 10, No. 1, (2009), 013001-013018.
14. Park, W.I. and Yi, G.C., "Electroluminescence in n-ZnO nanorod arrays vertically grown on p-GaN", ***Advanced Materials,*** Vol. 16, No. 1, (2004), 87-90.
15. Li, L. M., Du, Z.F., Li, C.C., Zhang, J. and Wang, T.H., "Ultralow threshold field emission from ZnO nanorod arrays grown on ZnO film at low temperature", ***Nanotechnology,*** Vol. 18, No. 35, (2007), 355606-355611.
16. Lockett, A.M., Thomas, P.J. and O'Brien, P., "Influence of seeding layers on the morphology, density, and critical dimensions of ZnO nanostructures grown by chemical bath deposition", ***Journal of Physical Chemistry C,*** Vol. 116, (2012), 8089–8094.
17. Liu, J.P., Huang, X.T., Li, Y.Y., Ji, X.X., Li, Z.K., He, X. and Sun, F.L., "Vertically aligned 1D ZnO nanostructures on bulk alloy substrates: direct solution synthesis, photoluminescence, and field emission", ***Journal of Physical Chemistry C,*** Vol. 111, (2007), 4990–4997.
18. Vayssieres, L., "Growth of arrayed nanorods and nanowires of ZnO from aqueous solutions", ***Advanced Materials,*** Vol. 15, (2003), 464-466.
19. Chen, L.Y., Yin, Y.T., Chen, C.H. and Chiou, J.W., "Influence of polyethyleneimine and ammonium on the growth of ZnO nanowires by hydrothermal method", ***The Journal of Physical Chemistry C,*** Vol. 115, (2011), 20913–20919.
20. Vanecek, M., Neykova, N., Babchenko, O., Purkrt, A., Poruba, A., Remes, Z., Holovsky, J., Hruska, K., Meier, J. and Kroll, U., "New 3-dimensional nanostructured thin film silicon solar cells", ***in: Proceedings of the 25th European Photovoltaic Solar Energy Conference,*** (2010), 2763–2766.
21. Kuang, Y., Werf, K.H.M., Houweling, Z.S. and Schropp,R.E.I., "Nanorod solar cell with an ultrathin a-Si: H absorber layer", ***Applied Physics Letters,*** Vol. 98, (2011), 113111/1-113111/3.
22. Malek, M.F., Sahdan, M.Z., Mamat, M.H., Musa, M.Z., Khusaimi, Z., Husairi, S.S., Md Sin, N.D. and Rusop M., "A novel fabrication of MEH-PPV/Al:ZnO nanorod arrays based ordered bulk heterojunction hybrid solar cells", ***Applied Surface Science,*** Vol. 275, (2013), 75– 83.
23. Olson, D.C., Lee, Y.J., White, M.S., Kopidakis, N., Shaheen, S.E., Ginley, D.S., Voigt, J.A. and Hsu, J.W.P., "Effect of polymer processing on the performance of poly(3-hexylthiophene)/ZnO nanorod photovoltaic devices", ***The Journal of Physical Chemistry C,*** Vol. 111, (2007), 16640–16645.
24. Takanezawa, K., Tajima, K. and Hashimoto, K., "Efficiency enhancement of polymer photovoltaic devices hybridized with ZnO nanorod arrays by the introduction of a vanadium oxide buffer layer", ***Applied Physics Letters,*** Vol. 93, (2008), 1–3.
25. Olson, D.C., Piris, J., Collins, R.T., Shaheen, S.E. and Ginley, D.S., "Hybrid photovoltaic devices of polymer and ZnO nanofiber composites", ***Thin Solid Films,*** Vol. 496, No. 1, (2006), 26–29.
26. Peiro, A.M., Ravirajan, P., Govender, K., Boyle, D.S., O'Brien,P., Bradley, D.D.C., Nelson, J. and Durrant, J.R., "Hybrid polymer/metal oxide solar cells based on ZnO columnar structures", ***Journal of Materials Chemistry,***Vol. 16, (2006), 2088–2096.
27. Peng, Z.A. and Peng, X., "Mechanisms of the Shape Evolution of CdSe Nanocrystals", ***Journal of The American Chemical Society,*** Vol. 123, No. 7, (2001), 1389-1395.
28. Yu, W.W., Qu, L.H., Guo, W.Z. and Peng, X.G., "Experimental Determination of the Extinction Coefficient of CdTe, CdSe, CdS Nanocrystals", ***Chemistry of Materials,*** Vol. 15, (2003), 2854-2860.
29. Lewis, N.S., "Toward Cost-Effective Solar Energy Use", ***Science,*** Vol. 315, (2007), 798-801.
30. Denzler, D., Olschewski, M. and Sattler, K., "Luminescence studies of localized gap states in colloidal ZnS nanocrystals", ***Journal of Applied Physics,*** Vol. 84, (1998), 2841– 2845.
31. Nasr, T. B., Kamoun, N. and Guasch, C., "Structure, surface composition, and electronic properties of zinc sulphide thin films", ***Materials Chemistry and Physics,*** Vol. 96, (2006), 84–89.
32. Deulkara, S.H., Bhosalea, C.H. and Sharonb, M., "A comparative study of structural, compositional, thermal and optical properties of non stoichiometric (Zn, Fe) S chalcogenide pellets and thin films", ***Journal of Physics and Chemistry of Solids,*** Vol. 65, (2004), 1879–1885.
33. Vidal, J., Melo, O., Vigil, O., Lopez, N., Contreras-Puente G. and Zelaya-Angel, O., "Influence of magnetic field and type of substrate on the growth of ZnS films by chemical bath", ***Thin Solid Films,*** Vol. 419, (2002), 118–123.
34. Elidrissi, B., Addou, M., Regragui, M., Bougrine, A., Kachouane, A. and Bernede, J. C., "Structure, composition and optical properties of ZnS thin films prepared by spray pyrolysis", ***Materials Chemistry and Physics,*** Vol. 68, (2001), 175-179.
35. Pathan, H.M. and Lokhande, C.D., "Deposition of metal chalcogenide thin films by successive ionic layer adsorption and reaction (SILAR) method", ***Bulletin of Materials Science,*** Vol. 27, No. 2, (2004), 85–111.
36. Joo, J., Kim, D., Yun, D.J., Jun, H., Rhee, S.W., Lee, J.S., Yong, K., Kim, S. and Jeon, S., "The fabrication of highly uniform ZnO/CdS core/shell structures using a spin-coating-based successive ion layer adsorption and reaction method", ***Nanotechnology,*** Vol. 21, (2010), 325604-325609.
37. Im, S.H., Kim, H.J. and Seok, S.I., "Near-infrared responsive PbS-sensitized photovoltaic photodetectors fabricated by the spin-assisted successive ionic layer adsorption and reaction method", ***Nanotechnology,*** Vol. 22, (2011) ,395502-395506.
38. Chen, Z. and Gao, L., "A facile route to ZnO nanorod arrays using wet chemical method", ***Journal of Crystal Growth,*** Vol. 293, (2006), 522–527.
39. Li, Q.C., Kumar, V., Li, Y., Zhang, H., Marks, T.J. and Chang, R.P.H., "Fabrication of ZnO nanorods and nanotubes in aqueous solutions", ***Chemistry of Material,*** Vol. 17, (2005), 1001-1006.

40. Hullavarad, S., Hullavarad, N., Look, D. and Claflin, B., "Persistent photoconductivity studies in nanostructured ZnO UV sensors", ***Nanoscale Research Letters,***Vol. 4, No. 12, (2009), 1421-1427.

41. Wang, Z.L., Kong, X.Y. and Zuo, J.M., "Induced Growth of Asymmetric Nanocantilever Arrays on Polar Surfaces", ***Physical Review Letters,*** Vol. 91, (2003), 18550/1-18550/4.

42. Shockley, W. and Queisser, H.J., "Detailed balance limit of efficiency of p–n junction solar cells***", Journal of Applied Physics,*** Vol. 32, No. 3, (1961), 510–519.

43. Nozik, A.J., "Quantum dot solar cells", ***Physica E,*** Vol. 14, (2002), 115–120.

44. Carlson, B., Leschkies, K., Aydil, E.S. and Zhu, X.Y., "Valence Band Alignment at Cadmium Selenide Quantum Dot and Zinc Oxide (1010) Interfaces", ***Journal of Physical Chemistry C,*** Vol. 112, (2008), 8419–8423.

45. Novoselov, K.S. and Castro Neto, A.H., "Two-dimensional crystals-based heterostructures: materials with tailored properties", ***Physica Scripta,*** Vol. 146, (2012) 014006 (6pp).

46. Dixit, S.K., Madan, S., Madhwal, D., Kumar, J., Singh, I., Bhatia, C.S., Bhatnagar, P.K. and Mathur, P.C., "Bulk heterojunction formation with induced concentration gradient from a bilayer structure of P3HT: CdSe/ZnS quantum dots using inter-diffusion process for developing high efficiency solar cell", ***Organic Electronics,*** Vol. 13, (2012), 710–714.

47. Lim, D. C., Shim, W.H., Kim, K.D., Seo, H.O., Lim, J.H., Jeong, Y., Kim, Y.D. and Lee, K., "Spontaneous formation of nanoripples on the surface of ZnO thin films as hole-blocking layer of inverted organic solar cells", ***Solar Energy Materials and Solar Cells,*** Vol. 95, (2011), 3036–3040.

48. Nikabadi, H.R., Shahtahmasebi, N., Rokn-Abadi, M.R., Bagheri Mohagheghi, M.M. and Goharshadi, E.K., "Gradual growth of gold nanoseeds on silica for SiO_2@gold homogeneous nano core/shell applications by the chemical reduction method", ***Physica Scripta,*** Vol. 87, (2013), 025802 (5pp).

49. Zhang, L., Qin, D., Yang, G. and Zhang, Q., "The investigation on synthesis and optical properties of ZnS:Co Nanocrystals by using hydrothermal method", ***Chalcogenide Letters,*** Vol. 9, (2012), 93-98.

50. Palve, A. M. and Garje, S. S., "A facile synthesis of ZnS nanocrystallites by pyrolysis of single molecule precursors, Zn (cinnamtscz)2 and $ZnCl_2$ (cinnamtsczH)$_2$", ***Bulletin of Materials Science,*** Vol. 34, (2011), 667–671.